Baker (2017), *Neuroimage*, **147**: 89-96
doi: 10.1016/j.neuroimage.2016.12.008

Decoding eye-of-origin outside of awareness

Daniel H. Baker
Department of Psychology, University of York, UK
email: daniel.baker@york.ac.uk

Abstract

In the primary visual cortex of many mammals, ocular dominance columns segregate information from the two eyes. Yet under controlled conditions, most human observers are unable to correctly report the eye to which a stimulus has been shown, indicating that this information is lost during subsequent processing. This study investigates whether eye-of-origin information is available in the pattern of electrophysiological activity evoked by visual stimuli, recorded using EEG and decoded using multivariate pattern analysis. Observers (N=24) viewed sine-wave grating and plaid stimuli of different orientations, shown to either the left or right eye (or both). Using a support vector machine, eye-of-origin could be decoded above chance at around 140 and 220ms post stimulus onset, yet observers were at chance for reporting this information. Other stimulus features, such as binocularity, orientation, spatial pattern, and the presence of interocular conflict (i.e. rivalry), could also be decoded using the same techniques, though all of these were perceptually discriminable above chance. A control analysis found no evidence to support the possibility that eye dominance was responsible for the eye-of-origin effects. These results support a structural explanation for multivariate decoding of electrophysiological signals – information organised in cortical columns can be decoded, even when observers are unaware of this information.

Keywords: MVPA; cortical columns; awareness; binocular vision.

1 Introduction

Signals from the left and right eyes remain anatomically segregated throughout the early stages of visual processing. In the primary visual cortex of most primates, cells that preferentially respond to signals from one or other eye are organised into ocular dominance columns (Adams et al., 2007; Horton and Hocking, 1996; Hubel and Wiesel, 1969). This striking columnar structure is lost at later stages of processing, when signals are combined binocularly to give a cyclopean percept of the world. When a visual stimulus is presented to only one eye under controlled conditions, humans generally lack explicit conscious awareness of which eye was stimulated ('utrocular discrimination', or more properly 'utrocular identification'; Ono and Barbeito, 1985). This loss of information is distinct from other visual cues, such as spatial position and orientation, that are also segregated anatomically, yet remain perceptually available to conscious awareness.

Recently, studies using electro- and magneto-encephalography (EEG and MEG) have shown that both simple (Cichy et al., 2015; Ramkumar et al., 2013; Wardle et al., 2016) and more complex (Carlson et al., 2013, 2011; Cichy et al., 2014; Coggan et al., 2016; Nemrodov et al., 2016) image properties can be decoded from the pattern of electromagnetic activity evoked by a visual stimulus. One study investigating orientation decoding (Cichy et al., 2015) has suggested that any information encoded in cortical columns should produce distinct spatial patterns of electrical activity that can be recovered using machine learning algorithms (multivariate pattern classifiers). Given the columnar representation of eye-of-origin in the early stages of cortical processing, this should extend to information about which eye (or combination of eyes) was stimulated, as has been demonstrated using fMRI (Schwarzkopf et al., 2010). Conversely, another recent study (Wardle et al., 2016) has claimed that the more perceptually distinct two stimuli are, the more easily their evoked responses can be dissociated using the same analysis techniques. This account would predict that eye-of-origin information should not be available in the electrophysiological evoked response, since it cannot be perceptually discriminated.

Here, sine-wave grating and plaid stimuli were presented to the left or right eye, as well as to both eyes together, whilst evoked responses were measured using EEG. For comparison with previous work, stimulus orientation was also manipulated, and conditions involving interocular conflict were included to probe the mechanisms of interocular suppression. To test the predictions of the two accounts of neural encoding described above, a support vector machine algorithm was trained to discriminate between the responses evoked by different combinations of the stimuli. The classifier achieved above-chance decoding accuracy for ocularity, orientation and pattern type, a finding not inconsistent with the idea that the cortical columnar structure for these cues results in different spatial patterns of evoked response that are apparent at the scalp. Observers were able to accurately report orientation, but not eye-of-origin, demonstrating that perceptual discriminability does not predict decoding accuracy across these ocular and spatial cues.

2 Methods

2.1 Observers

Written informed consent was obtained from 24 adults (8 male) with normal binocular vision. All observers wore their normal optical correction during testing if required. Experimental procedures were approved by the ethics committee of the Department of Psychology at the University of York.

2.2 Apparatus and stimuli

Stimuli were constructed from patches of sine-wave grating with a contrast of 50%, a spatial frequency of 2c/deg and a diameter of 10 degrees. Stimuli were in sine phase with the centre of the display. Two orientations (±45°) were presented either in isolation, or superimposed to form a plaid pattern. All stimuli were spatially windowed by a raised cosine envelope and had a small hole (1 degree in diameter) in the centre that was also blurred by a cosine ramp. Example stimuli are shown in Figure 1.

Stimuli were presented using a gamma corrected ViewPixx 3D display (VPixx Technologies, Canada). Binocular separation with minimal crosstalk was achieved by synchronising the refresh rate of the display with the toggling of a pair of active stereo shutter goggles (Nvidia Corp., California, USA) using an infra-red signal. The monitor refresh rate was 120Hz, meaning that each eye was updated at 60Hz.

EEG signals were recorded from 64 scalp locations from the 10-20 system using a WaveGuard cap and the ASAlab system (ANT Neuro, Netherlands). The ground was placed posterior to electrode *FPz*, and all channels were referenced to a whole-head average. Eye-blinks were recorded using vertical electro-oculogram electrodes. Stimulus onset was recorded on the EEG trace via low-latency digital triggers from the display device. Electrode impedances were typically kept below 10kΩ during testing, and signals were recorded at 1kHz and then stored for offline analysis.

2.3 Procedures

Stimuli were presented in 5 blocks, each comprising 220 trials (20 repetitions for each of the 11 conditions illustrated in Figure 1), and taking around 6 minutes. The stimulus duration was 100ms, and stimulus order was randomly determined in each block for each observer. After each stimulus presentation, observers indicated their percept using a two-button mouse, according to one of five different tasks (one task per block). In the first block, observers reported the stimulus orientation (tilted left or right). In the second block, they reported whether they saw one stimulus component (i.e. a single grating) or two components (i.e. a plaid or interocular conflict stimulus). In the third block, they reported whether they had seen the interocular conflict stimulus or another stimulus. In the final two blocks, observers were asked to indicate whether they believed one or two eyes had been stimulated (block four), and whether they believed the left or right eye had been stimulated (block five). Most observers found these final two tasks very difficult, and subsequently indicated that they were largely guessing throughout these blocks. In addition, they were instructed to guess when the stimulus did not clearly map onto the task (i.e. reporting the orientation of a plaid). Following each response, there was a variable length blank period (mean duration 1000ms, SD of 200ms) before the next stimulus was displayed. A central fixation cross was presented throughout.

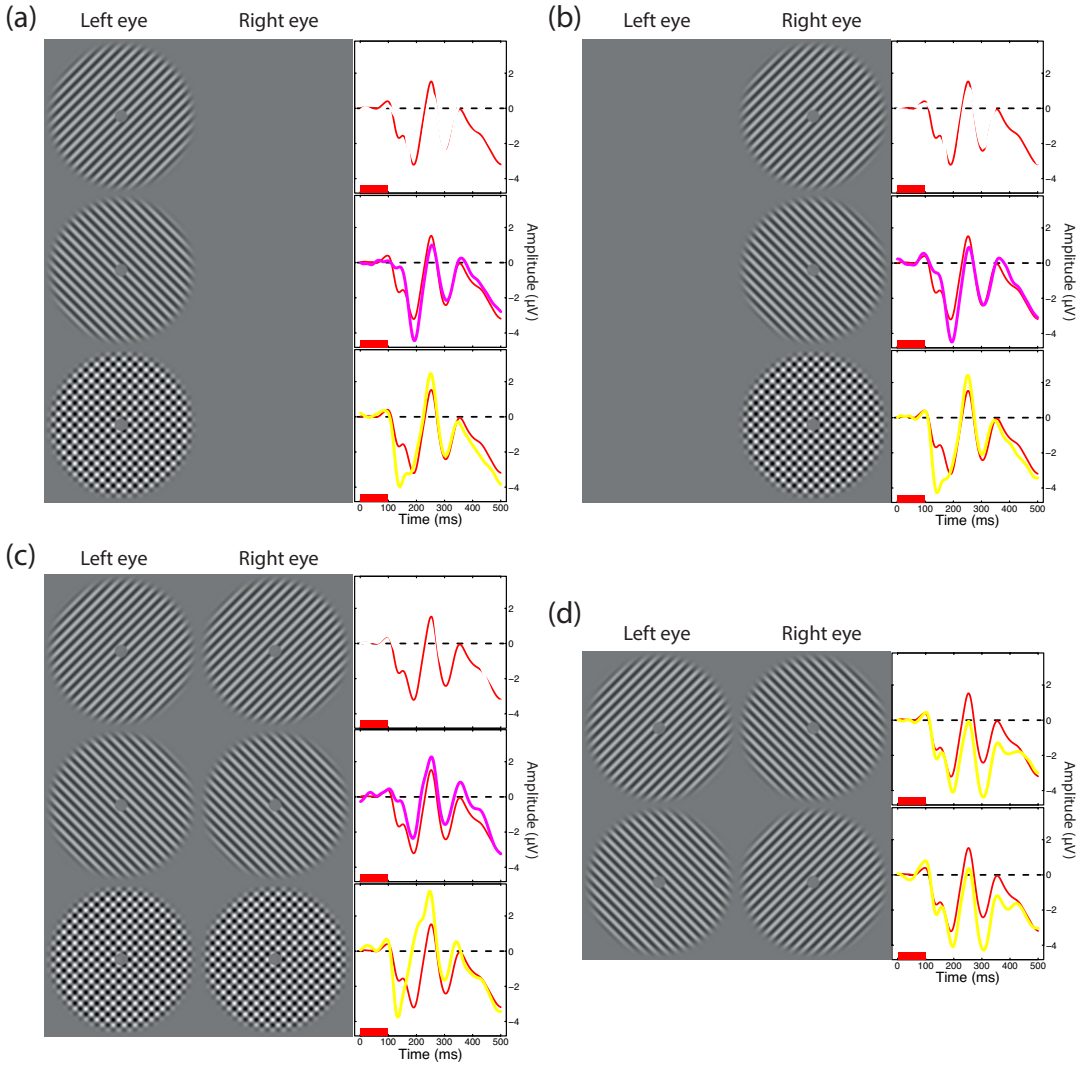

Figure 1: Example stimuli and averaged ERP waveforms for each condition. Panel (a) shows left eye stimuli and evoked responses, panel (b) shows right eye stimuli and evoked responses, panel (c) shows binocular stimuli and evoked responses, and panel (d) shows stimuli and evoked responses for the interocular conflict conditions. In each graph, the grey trace shows the grand average waveform across all 11 conditions for comparison. Each waveform is the average across 10 parieto-occipital electrode sites, 100 trials per observer, and 24 observers. The grey shaded rectangles in the lower left of each ERP plot indicate the period during which the stimulus was displayed.

EEG data were analysed offline. The data from each block were bandpass filtered between 0.01 and 30Hz, and trials were aggregated across blocks for each of the 11 conditions (see Figure 1; 100 trials per condition per observer). To calculate the ERPs in Figures 1 & 2, waveforms in the first 500ms following stimulus onset were normalized by the mean voltage in the 200ms time window before stimulus onset, and then averaged across ten occipito-parietal electrodes (Oz, O1, O2, POz, PO3-8), and then across trials and observers. No downsampling or artifact rejection was performed.

A support vector machine algorithm with a radial basis function kernel (Chang and Lin, 2011) was then trained to discriminate between the spatial patterns (i.e. the pattern of voltages across electrodes) of EEG response evoked by different combinations of stimuli, independently at each time point and for each observer. The classifier was trained on averages of random subsets of trials (means across 50 trials) from conditions of interest (see Figures 2 & 3), and its discrimination performance tested on the average of the remaining trials not included in the training. There were at least three examples for each condition in a comparison (depending on the total number

of conditions included in that comparison), and one example per condition for testing. The procedure was repeated 1000 times for each comparison (using different subsets of trials each time). The discrimination performance was then averaged across observers, and 95% confidence intervals were derived using bootstrap resampling to produce the timecourses in Figure 3b-d. The classifier was also trained and tested using the waveform across a time window (either 100-300ms in Figure 4, or in 100ms epochs for Figure S1) at each electrode independently to produce the scalp distributions in Figure 4.

A non-parametric cluster correction procedure (Maris and Oostenveld, 2007) was applied to determine significant clusters (either across time or across scalp locations) whilst controlling for multiple comparisons. For comparing ERP waveforms, summed *t*-values (from paired *t*-tests) across consecutive time points or adjacent electrode locations were compared with a null distribution generated by switching the condition labels for half of the observers. For assessing classifier accuracy, one-sample *t*-tests were used to compare accuracy to baseline (50% correct), and the null distribution was generated by reflecting half of the data points about the baseline (a procedure equivalent to changing the condition labels in a paired *t*-test). The cluster forming threshold was $t>2.069$, and the cluster significance threshold was $p<0.0083$ (i.e. $p<0.05$, Bonferroni corrected across the six comparisons under investigation). The entire cluster correction procedure was repeated for 1000 resampled data sets to derive confidence intervals for the onset and offset of significant clusters. Where resampled clusters did not overlap with significant clusters from the main data set they were discarded. Where multiple resampled clusters corresponded to a single original cluster, the onset of the first resampled cluster and the offset of the last resampled cluster were included in the resampled populations.

3 Results

All stimulus arrangements produced typical event-related potentials. Examples averaged across ten occipito-parietal electrodes (Oz, O1, O2, POz, PO3-8) are shown in Figure 1 for each condition, along with depictions of the stimulus arrangements. There were slight differences in the evoked potential across different conditions, with plaids (blue traces) producing earlier negative deflections than individual gratings (red and green traces), and binocular presentations (Figure 1c) evoking more generally positive responses than monocular presentations (Figure 1a,b). The interocular conflict conditions (Figure 1d) produced more generally negative responses than other conditions from around 150ms onwards.

The ERP waveforms for various combinations of conditions were averaged and compared statistically using cluster corrected paired *t*-tests. Comparing ERPs for stimuli (both gratings and plaids) presented to the left and right eyes (Figure 2a) revealed a very brief significant difference from 198–206ms post stimulus onset, and no significant clusters across the scalp in the 100-300ms time window. Comparing monocular and binocular presentation (Figure 2b) revealed that monocular stimuli evoked more negative voltages, with significant clusters from around 150-440ms, and across most of the scalp (with differences strongest at posterior electrodes). Comparing left- and right-tilted stimuli (Figure 2c) produced no significant differences. The remaining three comparisons (gratings vs plaids, Fig 2d; rivalry vs monocular plaids, Fig 2e; rivalry vs binocular gratings, Fig 2f) produced significant differences starting as early as 100ms, and persisting to around 400-500ms.

Baker (2017), *Neuroimage*, **147**: 89-96
doi: 10.1016/j.neuroimage.2016.12.008

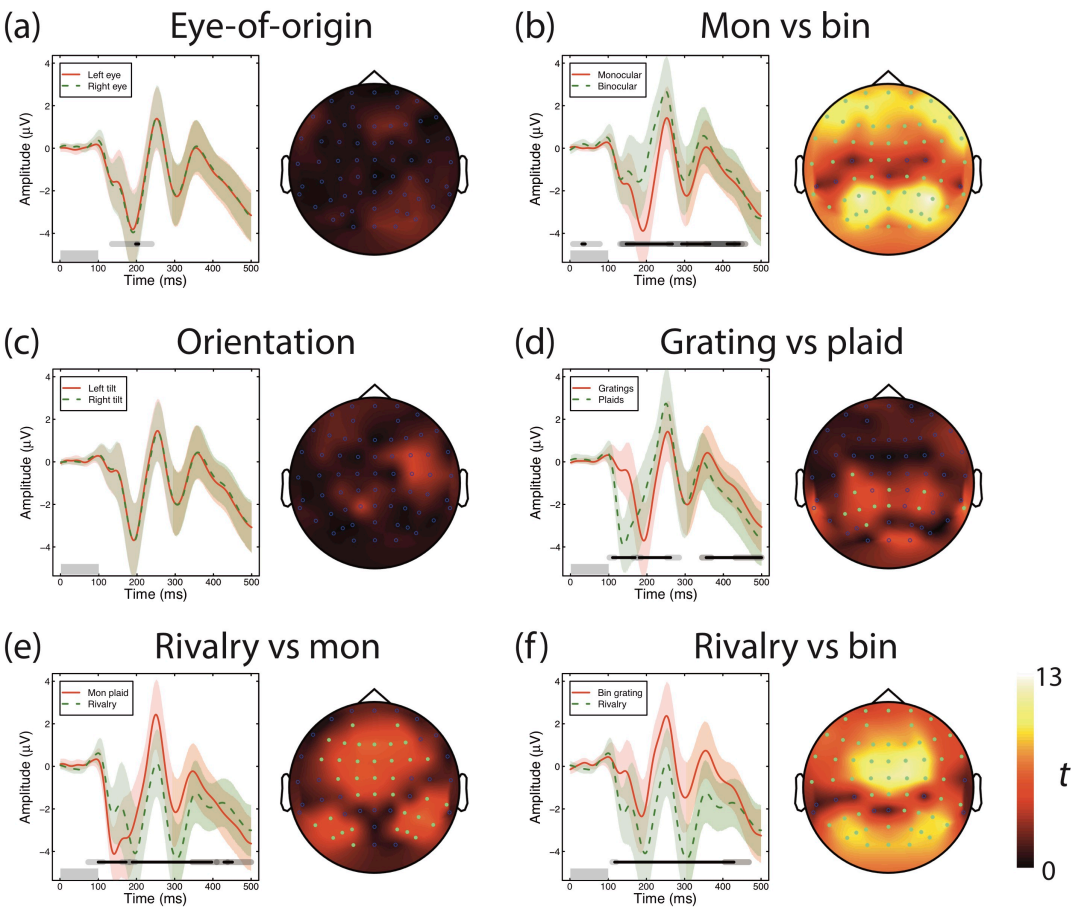

Figure 2: Comparison of stimulus-evoked potentials for different combinations of conditions during the 500ms following stimulus onset (curves, averaged across ten occipito-parietal electrodes) and in the time window from 100-300ms post stimulus onset (scalp plots). Black horizontal lines plotted at -4.5μV indicate cluster-corrected significant differences, with grey shaded regions indicating bootstrapped 95% confidence intervals. Red and green shaded regions give bootstrapped 95% confidence intervals of the mean across observers (N=24). Grey shaded rectangles along the x-axis indicate the time period when the stimulus was presented. In the scalp plots, intensity indicates the absolute *t*-statistic, scaled from black (t=0) to white (t=13), and green points highlight electrodes producing a cluster-corrected significant difference.

A support vector machine was then trained to discriminate between the patterns of electrical activity across the scalp produced by the same subsets of stimuli that were compared in Figure 2. The classifier was able to discriminate between stimuli (both gratings and plaids) shown to the left vs right eye (i.e. stimuli in Figure 1a compared with Figure 1b) at levels above chance from 134-148ms and 206-240ms following stimulus presentation (these time windows do not overlap with the significant cluster from Figure 2a). The maximum performance was 62% correct (solid red curve in Figure 3b). In contrast, the observers themselves were unable to report this information during the experiment, with left/right eye discrimination at 49% correct (where chance is 50%). Observers were slightly better (though by no means perfect) at reporting whether a stimulus was shown to one eye or two, averaging 64% correct for this task (see Figure 3a for a summary of the psychophysical responses). The classifier made this discrimination (i.e. stimuli in Figure 1a,b compared with Figure 1c) at above-chance levels from 90-345ms following stimulus onset, peaking at 80% correct (dashed green curve in Figure 3b).

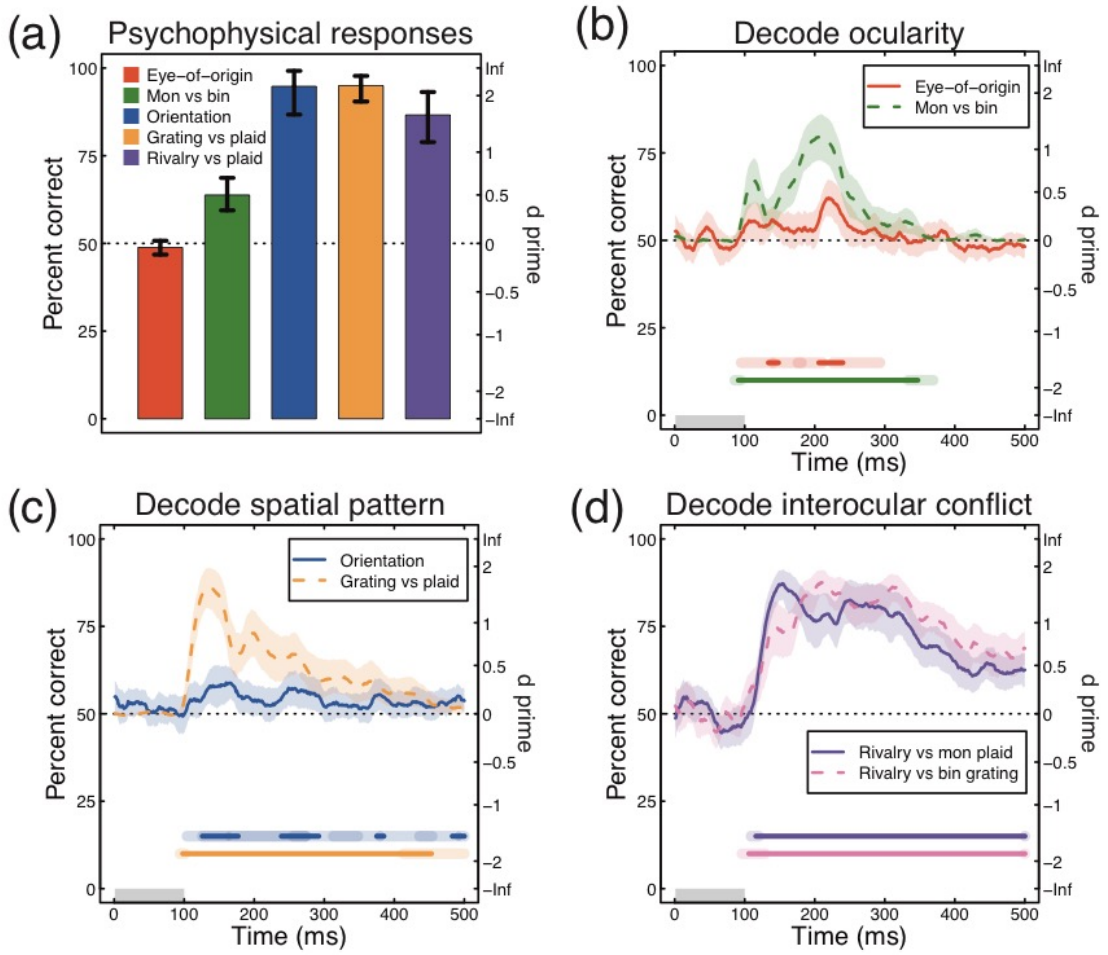

Figure 3: Summary of human and machine discrimination between different stimuli. Panel (a) shows a summary of psychophysical responses for five different discrimination tasks. Bonferroni-corrected one-sample *t*-tests revealed that eye-of-origin discrimination performance was not significantly different from chance, but all other discriminations were above chance (all $t>5$, all $p<0.01$, df=23). Panel (b) shows classifier performance for discriminating eye-of-origin (solid red curve), or monocular versus binocular presentation (dashed green curve). Panel (c) shows classifier performance for orientation (solid blue curve) and for discriminating gratings from plaids (dashed orange curve). Panel (d) shows classifier performance for discriminating the interocular conflict conditions from either a monocularly presented plaid (solid purple curve) or a binocularly presented grating (dashed pink curve). Error bars and coloured shaded regions in each panel give bootstrapped 95% confidence intervals (with 10000 resamples) of the mean across observers (N=24). Horizontal lines at the foot of each plot in panels b-d indicate periods of time when cluster-corrected *t*-tests were significantly above chance, with paler shaded regions giving bootstrapped confidence intervals. Grey shaded rectangles in panels b-d indicate the period during which the stimulus was displayed.

Since previous studies have reported above-chance decoding of pattern using similar techniques (Cichy et al., 2015), the data were then interrogated to assess how well spatial patterns could be discriminated. Human observers were able to report grating orientation (left/right tilt) with 95% accuracy, and discriminate gratings from plaids with 95% accuracy (blue and orange bars in Figure 3a). The classifier was relatively poor at decoding orientation, but did reach above-chance levels between 125-175ms and 240-290ms post stimulus onset, peaking at around 59% correct (blue curve in Figure 3c). Discriminating plaids from gratings was more successful, with performance above chance (peaking at 86% correct) in the time window from 100-450ms (orange dashed curve in Figure 3c).

Finally, the presence of a neural signature of interocular conflict was sought. The dichoptic conditions (Figure 1d) were compared with either a binocular grating (a comparison that holds constant the energy shown to the two eyes, and changes the orientation of one eye) or a monocular plaid (keeping the number of components fixed, and varying only eye of presentation for one component). Both of these comparisons

produced strong classifier performance (reaching maxima of 87% and 88% correct respectively) from 110ms until beyond the 500ms window used for the analysis (Figure 3d). Observers were able to discriminate interocular conflict from binocular and monocular plaids at 87% accuracy (purple bar in Figure 3a).

To determine which electrodes were most informative, further analyses were conducted in which the classifier was trained across a range of time points (from 100-300ms) for each individual electrode separately. Figure 4 shows classifier accuracy for this analysis plotted across the scalp. It is clear that for most comparisons the strongest contribution was from posterior electrodes near to early visual areas. This is consistent with the expectation that differences in the early visual evoked responses across conditions are able to support discrimination between stimuli. The interocular conflict and grating vs plaid conditions additionally produced strong decoding accuracy at more fronto-central electrodes, perhaps reflecting the longer timecourse over which classification was possible with these stimuli (see Figure 3d), and the salient perceptual differences they elicit (purple bar in Figure 3a). Expanding the analysis time window to the full 500ms post stimulus onset resulted in slightly lower classifier accuracy (as more noise was included), but approximately the same spatial pattern (not shown). The temporal evolution of scalp topographies in 100ms steps is shown in Supplementary Figure S1.

3.1 Influence of eye dominance

One possibility is that differences in ERP amplitude arising from eye dominance are responsible for the classifier performance in the eye-of-origin discrimination. If this were so, individuals with more extreme eye dominance should produce better decoding for this comparison because the dominant eye will evoke larger responses (Seyal et al., 1981). To derive a measure of eye dominance independently of the EEG data (thus avoiding 'double dipping'), psychophysical performance in the

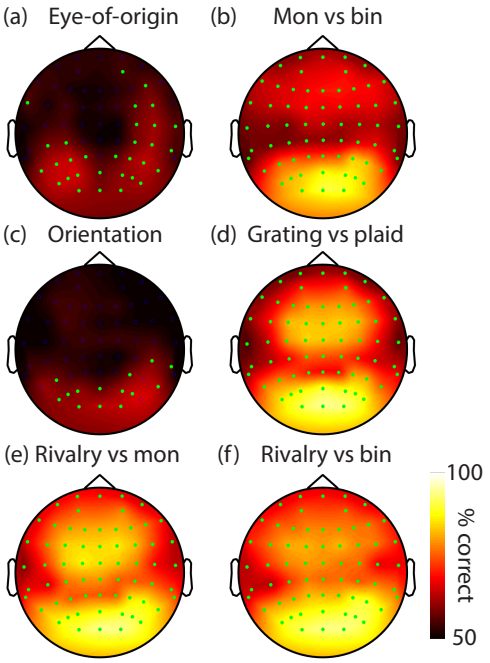

Figure 4: Scalp distribution of classifier accuracy from 100-300ms post stimulus onset, averaged across observers (N=24). Black regions reflect chance classifier accuracy (50% correct), white regions reflect perfect accuracy (100% correct). Green points indicate electrode locations where classifier performance remained significantly above chance following cluster correction.

orientation discrimination task for the interocular conflict conditions was used (Figure 1d). Individuals with a strong preference for the right eye will tend to perceive the stimulus presented to that eye more frequently than the stimulus presented to the left eye (e.g. Carter and Cavanagh, 2007; Mamassian and Goutcher, 2005), and therefore report seeing its orientation on the majority of trials. An eye dominance index was calculated for each observer using these data, and is shown in Figure 5a. The absolute value of this index (with values near 0 indicating good binocular balance, and values near 1 indicating strong eye dominance) was then correlated with individual classifier accuracy at each time point (Figure 5b). The lower bound of the bootstrapped confidence interval of this correlation did not exceed zero during the time window during which eye-of-origin could be decoded (red shaded regions). It is therefore unlikely that eye dominance is responsible for driving classifier performance.

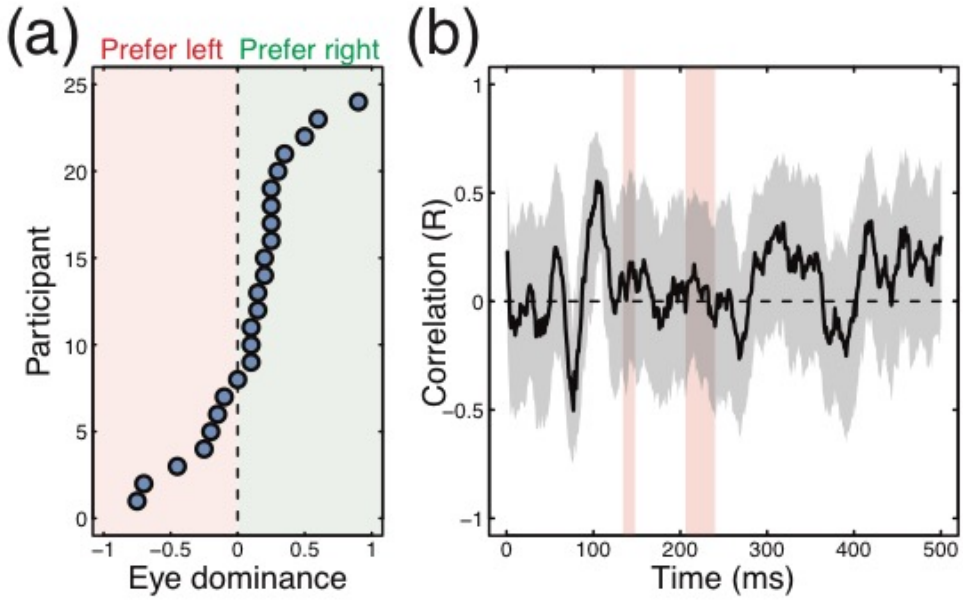

Figure 5: Eye dominance index (a) and correlation between eye dominance and classifier performance (b). In panel (a) each point represents an individual observer, sorted by eye dominance. Negative values indicate a preference for the left eye, positive values a preference for the right eye, with the majority of individuals being right eye dominant. Panel (b) shows the Pearson correlation coefficient between individual observers' absolute eye dominance index with their classifier performance in the eye-of-origin discrimination at each time point. The grey shaded region gives bootstrapped 95% confidence intervals of this correlation (10000 bootstrap resamples with replacement across observers). The red shaded regions indicate times at which eye-of-origin discrimination was significantly above chance (lower red lines from Figure 3b).

4 Discussion

Using multivariate pattern classification, eye-of-origin, binocularity and interocular conflict were all successfully decoded from EEG responses to simple visual stimuli. The observers performed at chance levels for discriminating eye-of-origin psychophysically, and were relatively poor (64% correct) at discriminating monocular from binocular presentation. Thus, the information encoding eye-of-origin (perhaps through anatomical organisation, such as cortical columns) that is available from electrophysiological responses must be subsequently lost to perception and consciousness. It was not possible to explain the classifier performance by considering the extent of eye dominance for individual observers, or from an amplitude difference in the ERP waveforms.

Classifier accuracy for eye-of-origin and orientation discrimination was markedly lower than for the other comparisons (Figures 3 & 4). These two comparisons also lacked significant differences between the mean ERP waveforms (Figure 2a,c; note that the significant cluster for the left vs right eye comparison occurred at a different time from the above-chance classifier accuracy). It is therefore likely that classifier accuracy in these conditions was not due to a mean univariate voltage difference, but instead represents differences in the detailed spatial pattern of electrical activity. The increased classifier performance for other conditions may be due to coarser amplitude differences between the waveforms (see Figure 2b,d,e,f). Interestingly, accuracy for discriminating orientation was lower than has been previously reported in studies using MEG instead of EEG (i.e. >90% correct, Cichy et al., 2015). This difference may be due to the increased signal-to-noise ratio of MEG compared with EEG, or the larger number of trials typically collected in previous studies (i.e. ~500 trials per condition, Cichy et al., 2015). Nevertheless, orientation discrimination performance was significantly above chance within the time window reported in previous studies, with comparable peak accuracy (59% correct) to other reports using similar numbers of trials (i.e. 67% correct with 100 trials per condition using MEG, Ramkumar et al., 2013).

Although observers in the present study were unable to accurately report eye-of-origin (red bar in Figure 3a), other studies have reported above-chance utrocular discrimination. However, there are often methodological problems that could explain this performance. For example, many studies used mirror stereoscopes and/or different displays for the two eyes. It is conceivable that alignment problems or luminance differences between the displays might provide spurious cues to eye-of-origin. Templeton & Green (1968) showed experimentally that proper control of convergence prevented above-chance utrocular discrimination performance. Ono and Barbeito (1985) performed experiments demonstrating that several spurious cues underpinning utrocular discrimination could be rendered unreliable, resulting in poor performance. In particular, introducing a luminance cue in the non-target eye reduces utrocular discrimination to chance (or below) in both stereo-normal and stereo-deficient observers (Barbeito et al., 1985).

In light of these potentially spurious cues, positive results can be viewed with some skepticism. For example, Blake & Cormack (1979) report differences across spatial frequency, with discrimination impossible at high frequencies (>4c/deg), but possible at lower frequencies for some observers. One explanation for this is that at lower frequencies a monocular luminance cue provides the eye-of-origin information. Schwarzkopf et al. (2010). reported accuracies of 57% correct at 0.5c/deg and 66% at 4c/deg, but observers were required to free-fuse the display, meaning that lapses in fusion would provide a spatial offset that cued eye-of-origin (Templeton and Green, 1968). In the present study, the stimuli were in sine-phase so were DC balanced (i.e. no luminance cue), and were displayed on a single monitor using shutter goggles, so that binocular fusion and vergence were natural. This arrangement produced chance performance on the utrocular discrimination task, implying that eye-of-origin information was lost to awareness.

Although utrocular discrimination under controlled conditions is not generally possible, it has been shown that eye-of-origin singletons can be identified in visual search experiments (Zhaoping, 2012). This suggests that information regarding salience, or perhaps information about *relative* eye-of-origin (same or different), could persist beyond the stage at which a 'labelled detector' (Watson and Robson, 1981) for explicit ocularity is lost. It is also apparent that observers had some ability to report whether a stimulus was monocular or binocular (64% correct, green bar in Figure 3a), even though these high contrast stimuli would likely appear identical in contrast (Baker et al., 2007). It therefore appears that humans have conscious access to information from their binocular visual system besides a mandatory binocular fusion of the two eyes' inputs. This information could include stereo depth from occlusion (McLoughlin and Grossberg, 1998), a binocular differencing channel (Li and Atick, 1994; May et al., 2012), or a 'lustre channel' that codes differences in luminance polarity across the eyes (Georgeson et al., 2016).

Decoding performance for the interocular conflict conditions was extremely good (>85% correct) and began around 110ms. The conflict conditions (in which the left and right eyes viewed gratings of different orientations) were compared to either a monocular plaid (where the number of components was the same, but both were shown to the same eye instead of different eyes) and to a binocular grating (where the number of eyes stimulated was the same, but both eyes saw the same orientation), with classifier performance being equally good for both comparison conditions. This is consistent with previous studies that have shown unique signatures of binocular rivalry in the ERP response over a similar time window (Jack et al., 2015; O'Shea et al., 2013). Interestingly, results using a different ERP paradigm (visual mismatch negativity) have been interpreted as evidence that eye-of-origin information persists during rivalry from around 100 to approximately 300ms (van Rhijn et al., 2013). This is consistent with the time window within which eye-of-origin could be decoded using monocular stimuli in the present study. However, it is possible that the ERP differences in the mismatch paradigm were due to a release from adaptation (because in the mismatch condition the orientations were switched between the eyes), and therefore be only incidentally encoding eye-of-origin. The paradigm used here provides a balanced design in which differences in the ERP are

due to differences in the response to identical stimuli shown to one or other eye (and not encoding a change in eye of presentation in a repeating stimulus sequence).

The source of the information used to decode orientation with MRI or MEG measures has provoked lively debate (Kamitani and Tong, 2005; Pratte et al., 2016; Swisher et al., 2010; summarised by Maloney, 2015). It has been suggested that decoding performance could be due to coarse-scale effects such as radial biases (Mannion et al., 2010), edge effects (Carlson, 2014), or differential allocation of attention (Alink et al., 2013). Some of these possibilities for orientation decoding using MEG have been ruled out by careful control experiments (Cichy et al., 2015), but might there be similar confounds for decoding eye-of-origin? In general there are fewer possible artifacts for eye-of-origin than for orientation, since the stimuli being discrminated are spatially identical. Coarser differences in the cortical representation of stimuli from the two eyes cannot be ruled out, but are not apparent histologically in the central 15° of the visual field (Adams et al., 2007) (the most obvious asymmetry, the blind spot, was far outside of the stimulus area). The presentation duration of 100ms is too brief for observers to plan and execute distinct eye movements to different stimuli, and eye-movement artefacts would likely be evident at anterior rather than the posterior electrodes that showed the strongest classifier performance (Figure 4a). Problems with accommodation, vergence and eye alignment might occur in some observers, but would likely be related to eye dominance effects that appear not to influence classifier performance (Figure 5). Regarding attention, the author is aware of no evidence that humans are able to deliberately allocate attention to one or other eye (apart from by winking).

Other studies have used MVPA of MEG data to explore how the neural response to a stimulus changes as a function of conscious awareness. Using a masking paradigm to suppress some stimuli from awareness, Salti et al. (2015) showed that visible and invisible stimuli are processed in the same way for the first 270ms, but additional responses then occur for visible stimuli in parietal and frontal regions. By masking numerical stimuli, Charles et al. (2014) demonstrated that perceptual responses did not depend on conscious awareness, but decoding of response accuracy was only possible for consciously perceived stimuli. The present study extends the use of MVPA beyond decoding stimuli that are suppressed from awareness, and shows that even for salient stimuli, some information that is lost to conscious awareness is still processed by the brain sufficiently to be decodable by MVPA.

Single unit work in macaque has demonstrated that the responses of most neurons in early visual areas during binocular rivalry are determined by the properties of the visual stimulus, rather than by the current percept (Leopold and Logothetis, 1996), whereas neurons in higher areas increasingly reflect perception (Logothetis and Schall, 1989). This suggests that responses in areas after binocular convergence still code information about monocular stimuli, and indeed this can be decoded from fMRI signals (Haynes and Rees, 2005). However in these paradigms there are always two stimuli in competition, and so the neural representation that is decoded might relate to stimulus characteristics (such as orientation or motion direction) that are merely correlated with eye-of-origin. In the present study, a single set of stimuli was displayed, and differed only in terms of the eye (or eyes) to which they were presented. Therefore, it is eye-of-origin, and not other aspects of the spatial pattern, that is being decoded.

4.1 Conclusions

This study has demonstrated that multivariate analysis of electrophysiological data can decode information about eye-of-origin that is not available to conscious perception. These findings are consistent with the recent claim (Cichy et al., 2015) that multivariate discrimination performance using such techniques reflects the brain's organisational structure, rather than perception (Wardle et al., 2016). The results also demonstrate that aspects of binocular processing, such as interocular conflict, evoke distinct patterns of electrical activity at the scalp.

5 Acknowledgements

Supported in part by the Wellcome Trust (ref: #105624) through the Centre for Chronic Diseases and Disorders (C2D2) at the University of York.

6 References

Adams, D.L., Sincich, L.C., Horton, J.C., 2007. Complete Pattern of Ocular Dominance Columns in Human Primary Visual Cortex. J. Neurosci. 27, 10391–10403. doi:10.1523/JNEUROSCI.2923-07.2007

Alink, A., Krugliak, A., Walther, A., Kriegeskorte, N., 2013. fMRI orientation decoding in V1 does not require global maps or globally coherent orientation stimuli. Front. Psychol. 4. doi:10.3389/fpsyg.2013.00493

Baker, D.H., Meese, T.S., Georgeson, M.A., 2007. Binocular interaction: contrast matching and contrast discrimination are predicted by the same model. Spat. Vis. 20, 397–413. doi:10.1163/156856807781503622

Barbeito, R., Levi, D., Klein, S., Loshin, D., Ono, H., 1985. Stereo-deficients and stereoblinds cannot make utrocular discriminations. Vision Res. 25, 1345–1348.

Blake, R., Cormack, R.H., 1979. On utrocular discrimination. Percept. Psychophys. 26, 53–68. doi:10.3758/BF03199861

Carlson, T.A., 2014. Orientation Decoding in Human Visual Cortex: New Insights from an Unbiased Perspective. J. Neurosci. 34, 8373–8383. doi:10.1523/JNEUROSCI.0548-14.2014

Carlson, T.A., Hogendoorn, H., Kanai, R., Mesik, J., Turret, J., 2011. High temporal resolution decoding of object position and category. J. Vis. 11(10), art 9. doi:10.1167/11.10.9

Carlson, T., Tovar, D.A., Alink, A., Kriegeskorte, N., 2013. Representational dynamics of object vision: The first 1000 ms. J. Vis. 13(10), art 1. doi:10.1167/13.10.1

Carter, O., Cavanagh, P., 2007. Onset rivalry: brief presentation isolates an early independent phase of perceptual competition. PloS One 2, e343. doi:10.1371/journal.pone.0000343

Chang, C.-C., Lin, C.-J., 2011. LIBSVM: A Library for Support Vector Machines. ACM Trans Intell Syst Technol 2, 27:1–27:27. doi:10.1145/1961189.1961199

Charles, L., King, J.-R., Dehaene, S., 2014. Decoding the Dynamics of Action, Intention, and Error Detection for Conscious and Subliminal Stimuli. J. Neurosci. 34, 1158–1170. doi:10.1523/JNEUROSCI.2465-13.2014

Cichy, R.M., Pantazis, D., Oliva, A., 2014. Resolving human object recognition in space and time. Nat. Neurosci. 17, 455–462. doi:10.1038/nn.3635

Cichy, R.M., Ramirez, F.M., Pantazis, D., 2015. Can visual information encoded in cortical columns be decoded from magnetoencephalography data in humans? NeuroImage 121, 193–204. doi:10.1016/j.neuroimage.2015.07.011

Coggan, D.D., Baker, D.H., Andrews, T.J., 2016. The role of visual and semantic properties in the emergence of category-specific patterns of neural response in the human brain. eNeuro 3(4): e0158-16.2016. 1-10.

Georgeson, M.A., Wallis, S.A., Meese, T.S., Baker, D.H., 2016. Contrast and lustre: a model that accounts for eleven different forms of contrast discrimination in binocular vision. Vision Res. 129: 98-118.

Haynes, J.-D., Rees, G., 2005. Predicting the Stream of Consciousness from Activity in Human Visual Cortex. Curr. Biol. 15, 1301–1307. doi:10.1016/j.cub.2005.06.026

Horton, J.C., Hocking, D.R., 1996. Anatomical demonstration of ocular dominance columns in striate cortex of the squirrel monkey. J. Neurosci. 16, 5510–5522.

Hubel, D.H., Wiesel, T.N., 1969. Anatomical demonstration of columns in the monkey striate cortex. Nature 221, 747–750.

Jack, B.N., Roeber, U., O'Shea, R.P., 2015. We make predictions about eye of origin of visual input: Visual mismatch negativity from binocular rivalry. J. Vis. 15(13), art 9. doi:10.1167/15.13.9

Kamitani, Y., Tong, F., 2005. Decoding the visual and subjective contents of the human brain. Nat. Neurosci. 8, 679–685. doi:10.1038/nn1444

Leopold, D.A., Logothetis, N.K., 1996. Activity changes in early visual cortex reflect monkeys' percepts during binocular rivalry. Nature 379, 549–553. doi:10.1038/379549a0

Li, Z., Atick, J.J., 1994. Efficient stereo coding in the multiscale representation. Netw. Comput. Neural Syst. 5, 157–174. doi:10.1088/0954-898X_5_2_003

Logothetis, N.K., Schall, J.D., 1989. Neuronal correlates of subjective visual perception. Science 245, 761–763.

Maloney, R.T., 2015. The basis of orientation decoding in human primary visual cortex: fine- or coarse-scale biases? J. Neurophysiol. 113, 1–3. doi:10.1152/jn.00196.2014

Mamassian, P., Goutcher, R., 2005. Temporal dynamics in bistable perception. J. Vis. 5, 361–375. doi:10.1167/5.4.7

Mannion, D.J., McDonald, J.S., Clifford, C.W.G., 2010. Orientation Anisotropies in Human Visual Cortex. J. Neurophysiol. 103, 3465–3471. doi:10.1152/jn.00190.2010

Maris, E., Oostenveld, R., 2007. Nonparametric statistical testing of EEG- and MEG-data. J. Neurosci. Methods 164, 177–190. doi:10.1016/j.jneumeth.2007.03.024

May, K.A., Zhaoping, L., Hibbard, P.B., 2012. Perceived Direction of Motion Determined by Adaptation to Static Binocular Images. Curr. Biol. 22, 28–32. doi:10.1016/j.cub.2011.11.025

McLoughlin, N.P., Grossberg, S., 1998. Cortical computation of stereo disparity. Vision Res. 38, 91–99.

Nemrodov, D., Niemeier, M., Mok, J.N.Y., Nestor, A., 2016. The time course of individual face recognition: A pattern analysis of ERP signals. NeuroImage 132, 469–476. doi:10.1016/j.neuroimage.2016.03.006

Ono, H., Barbeito, R., 1985. Utrocular discrimination is not sufficient for utrocular identification. Vision Res. 25, 289–299.

O'Shea, R.P., Kornmeier, J., Roeber, U., 2013. Predicting Visual Consciousness Electrophysiologically from Intermittent Binocular Rivalry. PLoS ONE 8, e76134. doi:10.1371/journal.pone.0076134

Pratte, M.S., Sy, J.L., Swisher, J.D., Tong, F., 2016. Radial bias is not necessary for orientation decoding. NeuroImage 127, 23–33. doi:10.1016/j.neuroimage.2015.11.066

Ramkumar, P., Jas, M., Pannasch, S., Hari, R., Parkkonen, L., 2013. Feature-Specific Information Processing Precedes Concerted Activation in Human Visual Cortex. J. Neurosci. 33, 7691–7699. doi:10.1523/JNEUROSCI.3905-12.2013

Salti, M., Monto, S., Charles, L., King, J.-R., Parkkonen, L., Dehaene, S., 2015. Distinct cortical codes and temporal dynamics for conscious and unconscious percepts. eLife 4. doi:10.7554/eLife.05652

Schwarzkopf, D.S., Schindler, A., Rees, G., 2010. Knowing with which eye we see: utrocular discrimination and eye-specific signals in human visual cortex. PloS One 5, e13775. doi:10.1371/journal.pone.0013775

Seyal, M., Sato, S., White, B.G., Porter, R.J., 1981. Visual evoked potentials and eye dominance. Electroencephalogr. Clin. Neurophysiol. 52, 424–428.

Swisher, J.D., Gatenby, J.C., Gore, J.C., Wolfe, B.A., Moon, C.-H., Kim, S.-G., Tong, F., 2010. Multiscale Pattern Analysis of Orientation-Selective Activity in the Primary Visual Cortex. J. Neurosci. 30, 325–330. doi:10.1523/JNEUROSCI.4811-09.2010

Templeton, W.B., Green, F.A., 1968. Chance results in utrocular discrimination. Q. J. Exp. Psychol. 20, 200–203. doi:10.1080/14640746808400150

van Rhijn, M., Roeber, U., O'Shea, R.P., 2013. Can eye of origin serve as a deviant? Visual mismatch negativity from binocular rivalry. Front. Hum. Neurosci. 7. doi:10.3389/fnhum.2013.00190

Wardle, S.G., Kriegeskorte, N., Grootswagers, T., Khaligh-Razavi, S.-M., Carlson, T.A., 2016. Perceptual similarity of visual patterns predicts dynamic neural activation patterns measured with MEG. NeuroImage 132, 59–70. doi:10.1016/j.neuroimage.2016.02.019

Watson, A.B., Robson, J.G., 1981. Discrimination at threshold: labelled detectors in human vision. Vision Res. 21, 1115–1122.

Zhaoping, L., 2012. Gaze capture by eye-of-origin singletons: interdependence with awareness. J. Vis. 12, 17. doi:10.1167/12.2.17

Baker (2017), *Neuroimage*, **147**: 89-96
doi: 10.1016/j.neuroimage.2016.12.008

7 Supplementary materials

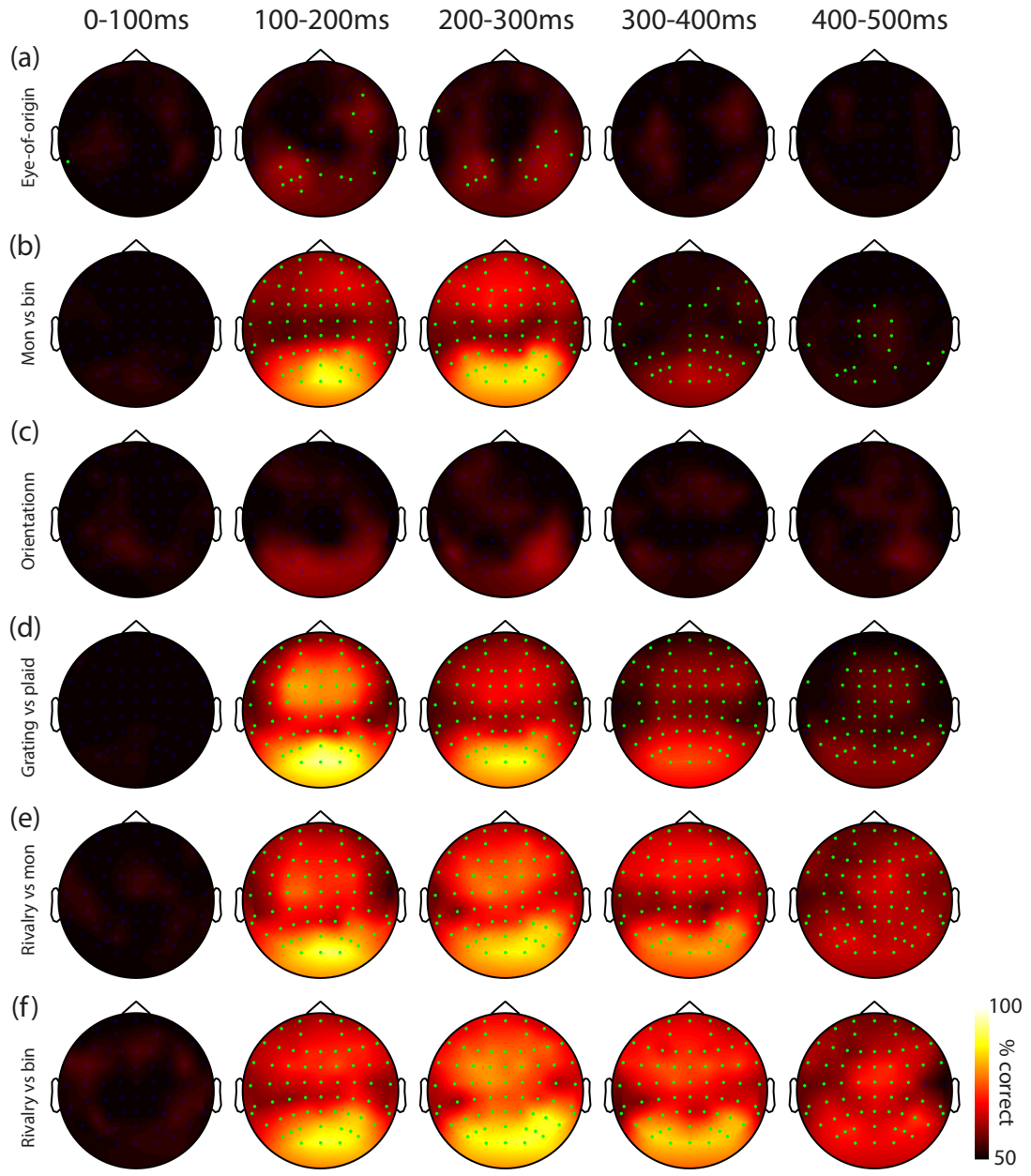

Figure S1: Scalp distributions of classifier accuracy in 100ms epochs for discriminating (a) eye of origin, (b) monocular vs binocular presentation, (c) orientation, (d) gratings vs plaids, (e) rivalry vs monocular plaids, (f) rivalry vs binocular gratings. Green points indicate electrodes that gave classifier performance that was significantly above chance following cluster correction.